HHS Public Access

Author manuscript

IEEE Trans Biomed Eng. Author manuscript; available in PMC 2016 January 01.

Published in final edited form as:

IEEE Trans Biomed Eng. 2016 January ; 63(1): 111–119. doi:10.1109/TBME.2015.2445713.

Chronic *in vivo* evaluation of PEDOT/CNT for stable neural recordings

Takashi D.Y. Kozai,
Department of Bioengineering, McGowan Institute of Regenerative Medicine, and Center for the Neural Basis for Cognition at the University of Pittsburgh, Pittsburgh, PA 15260

Kasey Catt,
Department of Bioengineering. University of Pittsburgh, Pittsburgh, PA 15260

Zhanhong Du,
Department of Bioengineering, McGowan Institute of Regenerative Medicine, and Center for the Neural Basis for Cognition at the University of Pittsburgh, Pittsburgh, PA 15260

Kyounghwan Na,
Department of Electrical Engineering, University of Michigan, Ann Arbor, MI

Onnop Srivannavit,
ePack, Inc in Ann Arbor, MI

Razi-ul M. Haque,
Structured Microsystems LLC in Ann Arbor, MI

John Seymour,
Department of Electrical Engineering, University of Michigan, Ann Arbor, MI

Kensall D Wise, **Euisik Yoon**, and
Department of Electrical Engineering, University of Michigan, Ann Arbor, MI

X. Tracy Cui
Department of Bioengineering, McGowan Institute of Regenerative Medicine, and Center for the Neural Basis for Cognition at the University of Pittsburgh, Pittsburgh, PA 15260

Takashi D.Y. Kozai: tdk18@pitt.edu; Zhanhong Du: tkozai@umich.edu; X. Tracy Cui: xic11@pitt.edu

Abstract

Objective—Sub-cellular sized chronically implanted recording electrodes have demonstrated significant improvement in single-unit (SU) yield over larger recording probes. Additional work expands on this initial success by combining the subcellular fiber-like lattice structures with the design space versatility of silicon microfabrication to further improve the signal-to-noise ratio, density of electrodes, and stability of recorded units over months to years. However, ultra-small microelectrodes present very high impedance, which must be lowered for SU recordings. While poly(3,4-ethylenedioxythiophene) (PEDOT) doped with polystyrene sulfonate (PSS) coating has demonstrated great success in acute to early-chronic studies for lowering the electrode impedance,

Correspondence to: Takashi D.Y. Kozai, tdk18@pitt.edu; X. Tracy Cui, xic11@pitt.edu.

concern exists over long-term stability. Here, we demonstrate a new blend of PEDOT doped with carboxyl functionalized multi-walled carbon nanotubes (CNTs) which shows dramatic improvement over the traditional PEDOT/PSS formula.

Methods—Lattice style subcellular electrode arrays were fabricated using previously established method. PEDOT was polymerized with carboxylic acid functionalized carbon nanotubes onto high impedance (8.0±0.1 MΩ: M±S.E.) 250 μm^2 gold recording sites.

Results—PEDOT/CNT coated subcellular electrodes demonstrated significant improvement in chronic spike recording stability over four months compared to PEDOT/PSS recording sites.

Conclusion—These results demonstrate great promise for subcellular sized recording and stimulation electrodes and long-term stability.

Significance—This project uses leading-edge biomaterials to develop chronic neural probes that are small (sub-cellular) with excellent electrical properties for stable long-term recordings. High density ultrasmall electrodes combined with advanced electrode surface modification are likely to make significant contributions to the development of long-term (permanent), high quality, and selective neural interfaces.

Index Terms

Conductive Polymer; Brain-computer interface; multi-electrode array; neuroprosthetics; Neural Interface

I. Introduction

Intracortical microelectrodes allow direct readout of brain signals. These devices are critical front-end components for the advancement of basic neuroscience knowledge including our understanding of behavior, decision-making, memory, plasticity, neural circuitry, connectivity, neurological diseases, and brain injuries [1, 2]. For chronic studies that examine training or learning, it is important that the system remains stable in order to identify that the neurological changes were due to neuroplasticity instead of an implant induced reactive tissue response. Microelectrode arrays have also been employed in human tetraplegia patients to restore functional motor control [3, 4]. The performance of these neural prosthetic system hinges largely on the ability of the device to record within quality, stability, and longevity requirements. The fundamental challenge is to develop advanced materials that will enable neural interface devices to remain functional and stable for as long as needed in the neural tissue.

Intracortical microelectrodes must be surgically implanted into the brain tissue. This insertion causes blood-brain barrier (BBB) injury which triggers a cascade of injury response pathways that lead to glial scarring and neural degeneration around the implanted electrodes [5–7]. While the insertion injury cannot be eliminated, studies have shown that subcellular sized, ultra-small lattices elicit significantly less glial scarring and neuronal loss [8]. Functionalized, sub-cellular sized carbon fiber based electrodes similarly showed reduce inflammatory response and significantly improved SU recording performance compared to silicon electrodes [9]. Recent, two-photon studies have also demonstrated reduced tissue

strain around sub-cellular sized electrodes due to reduced volumetric tissue displacement resulting from insertion [10]. These findings point to size as one key factor for improving chronic recording performance [11] (see review [5] for additional factors).

Reducing the implant size and recording site size, however, leads to an increase in impedance [9, 12]. While smaller recording sites improves the discrimination of SU waveform of the nearest neuron from other nearby action potential, the increased impedance leads to a decrease in the signal amplitude and increase in the noise floor. This makes the discrimination of action potentials from high amplitude noise increasingly difficult. To address these issues, conductive polymers have been employed to reduce the impedance of small, high impedance recording sites [9, 12–17]. These conductive polymers improve the charge transfer properties of the electrode-electrolyte interface in part by increasing the electrochemical surface area while maintaining the geometric surface area [18].

Several conductive polymers with good tissue biocompatibility properties exist, such as polypyrrole and polyaniline [18], among which PEDOT remains the most stable conductive polymer available for implantable devices. Still, the stability of PEDOT is heavily dependent on the dopant or counter-ion, concentration, ratio, and deposition parameters [18]. One way to further improve the stability of PEDOT is to modify the dopant. Carbon nanotubes are highly stable and intrinsically conductive dopants that improve the electrochemical stability of PEDOT beyond the stability of PEDOT/PSS, even under electrical stimulation [19, 20]. One concern of PEDOT/CNT is the biocompatibility of the coating, particularly if loose CNTs are shed from the coating. However, early chronic *in vivo* studies have indicated good biocompatibility of the coating, even with extended electrical stimulation [21].

Here, we explore the use of carbon nanotube doped PEDOT for chronic neural recording on novel ultra-small silicon lattice electrodes. For the CNT to act as a counter-ion during electrochemical deposition, it was necessary for the CNTs to be negatively charged. This is in contrast to non-charged CNTs that are passively entrapped into PEDOT/PSS during deposition (PEDOT/PSS:CNT) [22, 23]. CNTs were functionalized with negatively charged carboxylic acid using acid treatment and sonication [24]. The negatively charged CNTs replaced the need for PSS co-dopant and allows for greater CNT incorporation into the electrochemically deposited film. PEDOT/CNT-$(COOH)_x$ was electrochemically deposited onto small, high-impedance recording sites. These devices were implanted at least 12 weeks in mice primary visual cortex. The results showed PEDOT/CNT-$(COOH)_x$ coated recording sites dramatically outperformed PEDOT/PSS recording sites after 8 weeks.

II. Materials and Methods

A. Silicon Probe Fabrication

A custom 3.6 mm 2×4 design was desired for these experiments so photolithographically-defined neural probes were manufactured for this purpose using a slight modification to a well-defined silicon microfabrication process [25]. Silicon substrates were defined using boron-doping and diffusion. The trace material was polysilicon and the electrode material was Au because of its known compatibility with PEDOT electrodeposition [12]. Each site

area was 250 μm^2 or 18 μm in diameter. Intershank distance was 500 μm from centerline to centerline. Each lattice strut was 15μm wide and each shank was 55 μm wide and 3.6 mm long. The first recording site was 850 μm from the tip and three other sites were spaced at 116 μm. Windows in the lattices were 94 μm long and 25 μm wide every 116 μm. Recording sites with initial impedance values greater than 130 MΩ were considered open circuit due to poor wire bonding contacts to the print-circuit board and removed from the study prior to insertion.

B. Conductive Polymer Deposition

For PEDOT/PSS (N=21 sites), 0.1 M PSS (Acros Organics: 70,000 MW) and 0.01 M EDOT (Bayer) was dissolved in Millipore filtered diH_20 overnight on a stir-plate without shaking at 4 °C. Electrochemical deposition was conducted in galvanostatic mode at 500 pA for 500 s using a platinum foil counter electrode and a Ag/AgCl reference electrode.

CNTs were functionalized prior to deposition on the probes. The CNTs were functionalized with carboxylic acid groups by mixing 200mg of multi-walled carbon nanotubes into 25ml of concentrated nitric acid and 75ml concentrated sulfuric acid. This solution was sonicated for 2 hours and then vigorously stirred overnight at room temperature. The solution was then ultracentrifuged at 16k-rpm for 1 hr at 4 °C and the solute was poured off for pH test. Precipitate CNT-$(COOH)_x$s were resuspended in Millipore filtered diH2O and the ultracentrifugation process was repeated until the removed solution became pH neutral. Samples were then dried at 60°C.

For PEDOT/CNT-$(COOH)_x$ deposition (n=15 sites), 1mg of CNT-$(COOH)_x$ was resuspended in 1ml of diH2O by sonication for 10 minutes. EDOT was added to this solution to a concentration of 0.02M. Electrochemical deposition was conducted in galvanostatic mode at 500 pA for 500 s using a platinum foil counter electrode and a Ag/AgCl reference electrode. Electrodes for chronic implantation were ethylene oxide sterilized at least one week prior to electrode surgery. Samples for the SEM were imaged using a JSM 6330F SEM (JEOL, Japan) at an accelerating voltage of 3kV. Working distance was adjusted automatically to allow for optimal image quality (Fig. 2).

C. Surgical Implant Procedure

Surgical implant was conducted as extensively described in a previous publication [1]. Briefly, a coated array was implanted unilaterally into the left primary monocular visual cortex, (V1m: +1 mm lambda, +1.5 mm midline) of 5 male C57BL/6J mice under 1.5% isoflurane. Arrays were inserted at ~2 mm/s using a stereotaxic manipulator such that the top recording sites were at a depth of 500 μm. Local field potential (LFP) and current source density (CSD) were used to validate that the electrode sites were implanted into Layer IV and V [1]. The silicon device and the craniotomy were sealed carefully with silicone (Kwik-sil) and a headcap was created using UV-cured dental cement (Pentron Clinical, Orange CA). 5 mg/kg ketofen was administered daily for three days as a post-operative analgesic. All animal care and procedures were performed under the approval of the University of Pittsburgh Institutional Animal Care and Use Committee and in accordance with regulations specified by the Division of Laboratory Animal Resources.

D. Neural Recording and Analysis

Electrophysiological recording, single-unit (SU) analysis, and multi-unit (MU) analysis were conducted as extensively described in a previous publication (Fig. 3) [1]. Briefly, spontaneous recording was conducted in a dark room. Visual stimuli was presented using the MATLAB-based Psychophysics toolbox [26–28] on a 24" LCD (V243H, Acer. Xizhi, New Taipei City, Taiwan), while the animal was under isoflurane anesthesia. Solid black and white bar gratings were presented drifting in a perpendicular direction and synchronized with the recording system (RX7, Tucker-Davis Technologies, Alachua FL) at 24,414 Hz. The spike data stream was further pre-processed using published methods [29, 30]. Possible spikes were detected using a fixed negative threshold value of 3.5 SD. Offline spike sorting was carried out using a custom MATLAB script modified from previously published methods[9, 31].

The SU signal quality was defined as signal-to-noise amplitude ratio (SNAR), and was calculated as the peak-to-peak amplitude of the mean waveform of the cluster divided by twice the standard deviation of the noise:

$$SUSNAR = \mu_{SU-pp} \Big/ 2\sigma_{Noise} \quad (1)$$

where μ_{SU-pp} is the mean peak-to-peak amplitude of the waveform snippets and σ_{Noise} is the standard deviation of the spike data stream *after* all waveform snippets have been removed. If no SU was detected, SNAR was considered to be 0. This was done to prevent misleading over characterization of 'AVERAGE SNR' by ignoring or removing 'failed' recording sites during averaging. Only channels exhibiting sortable SU spikes with SNR >2 were analyzed. Candidate SU with SNR between 2 and 3 were manually confirmed or excluded by examining the combination of waveform shape, auto-correlogram, peak threshold crossing offset, and peristimulus time histogram (PSTH) with 50 ms bins. Candidate units with SNR below 2 were discarded, and candidate units with SNR greater than 3 were manually confirmed by examining the waveform shape.

For MU analysis, all spikes crossing the 3.5 SD threshold were used [32]. Multi-unit Signal-to-Noise Firing Rate Ratio (SNFRR) was defined as the average firing rate in a 550 ms bin of the 'ON' state minus the average firing rate of the 'OFF' state in a 550 ms bin after a 50 ms latency delay following the trigger divided by the average standard deviation of both the 'ON' and 'OFF' state.

$$MUSNFRR_{ON:OFF} = \frac{\mu_{on} - \mu_{off}}{\frac{1}{2}(\sigma_{on} + \sigma_{off})} \quad (2)$$

where μ_{on} and μ_{off} are the mean MU firing rate of the 'ON' and 'OFF' state, respectively, while σ_{on} and σ_{off} are the standard deviation of firing rates during the 'ON' or 'OFF' state, respectively. Two-sided Welch's T-test with the assumption of unequal variance and a p-value < 0.05 was conducted between 'ON' and 'OFF' firing rates. If no significant multi-unit was detected, MU amplitude and SNFRR were considered to be 0. This was done to

prevent misleading over characterization of ‘AVERAGE SNR’ by ignoring or removing ‘failed’ recording sites during averaging.

While SU signal strength can be quantified as the average voltage amplitude of the largest sorted single-unit, threshold-crossing events which include MU were a mixture of possible SUs with various amplitudes. Therefore MU signal strength of the largest reliable MU amplitude was estimated using the quality metric defined as

$$MU\,Amplitude = \mu_{MU-pp} + 2\sigma_{MU-pp} \quad (3)$$

where μ_{MU-pp} and σ_{MU-pp} are the mean peak-to-peak amplitude of and standard deviation of all of the waveform snippets, respectively. That is, the strength of the multiunit signal is defined as the average peak-to-peak MU amplitude plus two standard deviations of the standard deviation of all MU peak-to-peak amplitude.

E. Impedance Measurements

Electrochemical impedance was measured immediately after each neural recording session. While under anesthesia, the implanted array was connected to an Autolab potentiostat using a 16 channel multiplexer. Impedance was measured for each of the 8-channels using a 10 mV RMS sine wave from 10 Hz to 32 kHz, employing a 15 multisine paradigm to shorten the time required for measurement. In this work, the 1 kHz impedance is reported unless indicated otherwise.

III. Results

PEDOT with different counter ions were electrochemically deposited onto gold recording sites with a mean 1kHz impedance of 7,958±112 kΩ. PEDOT/PSS reduced the 1kHz impedance to 97.1±1.1 kΩ while PEDOT/CNT-$(COOH)_x$ reduced it to 90.3 ± 8.1 kΩ. SEM revealed the PEDOT/CNT-$(COOH)_x$ had a distinct and dense nanotube matrix structure that was significantly more porous than PEDOT/PSS. The coated electrodes were chronically implanted into the visual cortex of mice for SU and MU anlaysis.

A. Spike recording performance

The chronic SU and MU recording performance were evaluated in the visual cortex of mice (Fig. 3). Neural activity in the visual cortex was driven by stimulating the contralateral eye with drifting solid gratings.

The SU yield and MU yield started at similar values for both PEDOT/PSS and PEDOT/CNT (Fig. 4ab). While the SU yield for PEDOT/CNT coated sites held steady at around 50% throughout the implant, the SU yield on the PEDOT/PSS recording sites began dramatically decreased after the first month. Interestingly, the SU and MU yield for the PEDOT/CNT recording sites were identical. This indicates that PEDOT/CNT sites were able to detect clean SU waveforms on all recording sites detecting visually evoked neural activity. This, in turn, suggests good recording properties for isolating SUs from distant background units. In contrast, the PEDOT/PSS showed slightly better MU yield than SU yield. However, the MU yield of PEDOT/PSS also decreased dramatically after the first 1–2 months.

SU SNAR, SU amplitude and MU amplitude were similar on the day of surgery (Fig. 4c–f). For PEDOT/CNT, SU SNAR was initially 3.0±0.6 and SU amplitude was 78.3±15.2 μV, while for PEDOT/PSS they were 2.1±0.4 and SU amplitude was 50.6±11.2 μV. Interestingly, on the day of the surgery, MU SNFRR was significantly better for PEDOT/PSS at 0.47±0.08 compared to 0.16±0.03 for PEDOT/CNT. For the first 42 days, PEDOT/PSS performed similarly to previously published results [9, 13] and statistically similarly to PEDOT/CNT. However, 7–8 weeks after implantation, the performance of PEDOT/PSS recording sites are significantly ($p<0.05$) lower than the PEDOT/CNT sites. While the original study was intended for 12 wks (84 days), PEDOT/CNT recordings were extended due to its continuously strong recording performance.

B. Chronic Impedance

The impedance of PEDOT/CNT recordings sites steadily increased for the first three months, then stabilized (Fig. 5). In contrast, PEDOT/PSS recording sites increased for the first 2 weeks, then decreased over the next two weeks before steadily increasing (Fig. 5). Most interesting is that during day 7 and day 14, when the impedance of PEDOT/PSS was greater than PEDOT/CNT, the noise floor of PEDOT/PSS were significantly lower than PEDOT/CNT ($p<0.05$). There was no trending difference in noise floor during the second month, while PEDOT/CNT had a lower noise floor than PEDOT/PSS during the 3rd month. It should be noted that while impedance and noise floor may provide supplemental information, our previous data show they are poor predictors of recording performance [1, 10, 32].

IV. Discussion

In this study, two PEDOT blends were compared for chronic recordings; the more commonly used PEDOT/PSS (PSS MW 70,000Da) and PEDOT/CNT. Both blends were deposited under galvanostatic mode with the same current level and total deposition charge. All devices were implanted into the same anatomical coordinates including depth and the recording sites were confirmed to remain in Layers IV and V throughout the duration of the study using CSD. The chronic recording performance of PEDOT/PSS remains comparable for the first 5–6 wks which are supported by previous early chronic studies [9, 13]. Although the acute insertion injury related inflammation stabilizes in the first few weeks, the chronic tissue response continues to evolve for many months [10]. In fact, chronically implanted PEDOT/CNT coated Au recording sites significantly out preformed PEDOT/PSS recording sites after 7–8 wks following implantation.

Interestingly, the 1 kHz impedance of the PEDOT/PSS increased over the first couple of weeks, then decreased before steadily increasing. When the recording performance began to significantly degrade, the impedance value was 988±121 kΩ. In contrast, PEDOT/CNT steadily increased, up to 2,511±67 kΩ but the increase in impedance did not dramatically impact recording performance. As discussed in previous studies, the 1 kHz impedance magnitude does not linearly correlate with quality of recording. The higher quality and longer lasting recording from the PEDOT/CNT may be a result of the better tissue integration of the nanofibrous and porous sites with the host tissue. The intimate integration

leads to close proximity between the neuron and the recording sites. The initial more rapid increase of the impedance of PEDOT/PSS suggests higher degree of inflammatory tissue reaction, which could lead to reduced neuronal density around the PEDOT/PSS sites. The impedance of the PEDOT/CNT steadily increase over time until around 10 weeks, the reason for this increase is not known but may be a result of protein and tissue filling into the pores of the PEDOT/CNT film which reduces the effective surface area. In another study when we were able to retrieve the PEDOT/CNT coated implants, such phenomenon was observed (Data not shown). On the other hand, PEDOT/PSS's sharp impedance increase and decrease at acute time suggest a more aggressive cellular tissue response. The more steady increase of impedance after three weeks may be a result of fouling or degradation of the mechanical/chemical stability.

However, additional research is necessary to determine if the significant differences in performance is due to the coating's impact on changes in material property. More detailed equivalent circuit analysis may help to test these hypotheses. Previous histological study demonstrated that prolonged electrical stimulation through PEDOT:CNT coated electrodes did not lead to significant differences in the quantitative histology [21]. This suggests the coating did not exacerbate the reactive tissue response, for example through the shedding of loose CNT during stimulation. It is expected that passive recording through the coating will have reduced inflammation compared to when electrically stimulated [18]. However, it should be noted that while impedance and post-mortem histology may supplement recording data, they are poor predictors of recording quality [10]. Therefore, PEDOT/PSS and PEDOT/CNT coatings were compared across single-unit and functional evoked multi-unit recording performance metrics. Particularly, the ability to record visually evoked multi-unit firing rate changes suggest that the neurons being recorded remain integrated in the primary visual neural circuit and are relatively healthy. While additional research is needed to better understand *in vivo* failure mechanisms of conductive polymers, opportunities still exist for improving their chronic *in vivo* stability.

The center and edge recording sites were also compared. However, neither a significant difference nor even a trending difference was observed. While additional research may be necessary, it is possible that at small lattice dimensions (<55×15 μm) there is minimal impact on recording site location. While other groups have compared recording performances of different devices in the literature [33–36], additional research is necessary to compare recording performance of these devices to PEDOT/CNT coated commercially available devices. To percisely compare recording performance across devices, visually evoked chronic recording performance must be collected in the primary monocular visual cortex of mice at layer IV and V over 6 months with PEDOT/CNT coated devices. This data is not currently available from the literature. These are, however, beyond the scope of this study of comparing chronic recording performance of PEDOT/CNT and PEDOT/PSS electrode sites, which showed significant differences after 7–8 weeks post implantation.

PEDOT has gained substantial popularity for improving the electrical property of implantable devices. It is relatively simple to polymerize under a wide range of deposition parameters, concentrations, electrode size, and electrode shape. However, the wide range of PEDOT polymerization also results in a wide range of electrical and mechanical stabilities.

Furthermore, EDOT is an organic liquid, and the method used to dissolve it into water impacts its effective concentration during deposition (e.g. stirring for 8 hrs vs vortexing for 10 min). Poor understanding of how these variables impact PEDOT stability has led to the concern that PEDOT cannot be electrically stable longitudinally *in vivo*.

To date, PEDOT remains the most stable conductive polymer available for implantable devices. These results demonstrate that the stability of PEDOT can be improved by tuning the dopant or counter-ion. Further optimization of concentration, ratio, and deposition parameters, such as chemical deposition or electrochemical deposition may improve the PEDOT stability [18]. For example, electrochemical deposition can also be altered by using potentiostatic or galvanostatic mode. Current density or charge density and total deposition charge can also influence the thickness and stability of the coating.

Carbon has nearly an order of magnitude higher capacitive charge transfer capacity, as well as over 8 orders of magnitude greater resistance than traditional metals, which makes the electrode site resilient to damage from Faradaic charge transfer [37]. This property has previously been shown to improve the electrode material against electrical stimulation [19, 20]. In addition, carbon has been shown to possess photoelectric/photothermal neural stimulation properties [38]. With CNTs, these properties can also be fine-tuned. CNTs come in a wide variety of lengths, outer diameter, inner diameter, (n,m) index, dopants, number of walls (e.g. single-walled, double-walled, triple-walled, multi-walled), and whether the ends of the tubes are opened or closed. The (n,m) index orientation (i.e. the orientation of the graphene honeycomb in the tube) can alter the bandgap of the CNT [e.g. metallic (n = m), quasi-metallic (n−m = 3X, where X is an integer), semiconducting (others)].

In order to achieve a high density of CNTs in the PEDOT matrix, it was necessary to add negatively charges to the CNTs [19]. This was done using strong acid treatments and sonication to add carboxylic acid functional groups to the CNTs. The resulting PEDOT structure was a dense lattice matrix structure held in place by the PEDOT conductive polymer. The ultrastucture of the negatively charged CNT incorporated PEDOT was much more porous and contained higher density of CNTs than the PEDOT/PSS with neutral CNT diffused PEDOT/PSS+CNT [22, 23]. Furthermore, hollow CNTs can be functionalized with surface chemistry or employed as a reservoir for controlled-release local drug delivery [39].

V. Conclusion

Emerging research points to sub-cellular sized devices as significantly improve chronic electrophysiology recording performance. As the microelectrodes get smaller, recording sites also need to become smaller. Smaller recording sites, further improves the ability to isolate single-unit waveforms from distant neurons, but tend to result in high electrical impedance. PEDOT has gained rapid popularity as an electrode site coating to improve electrical properties of the site with many classes of implantable devices due to its ease of use. The rapid adoption of this technology without careful calibration of deposition parameter to optimize stability for each electrode type and size has exacerbated the concern that PEDOT is inherently unstable and cannot be used for chronic applications. Here we demonstrate that the stability of PEDOT can be reinforced using CNTs to significantly

improve chronic recording performance after 50 days post-implant. CNTs further add functionality to implantable devices, including the capacity for drug delivery. The enhanced recording performance demonstrates promising results for improving conductive polymer coated sites for implantable devices. Lastly, PEDOT/CNT coatings are not limited to ultrasmall electrodes, but may be applied to a broad electrode design space including microwire, Michigan, and Utah Arrays.

Acknowledgment

Device design, fabrication, and packaging were funded by DARPA RE-NET RCI MTO Contract No. N66001-12-C-4022. For the microfabrication work, we gratefully acknowledge the use of the Lurie Nanofabrication Facility at the University of Michigan and the support of LNF staff members. Animal study was supported by NINDS 5R01 NS062019 and seed funding from the Department of Bioengineering and the Brain Institute at the University of Pittsburgh. SEM was conducted at the University of Pittsburgh Center for Biological Imaging.

References

1. Kozai TDY, et al. Comprehensive chronic laminar single-unit, multi-unit, and local field potential recording performance with planar single shank electrode arrays. Journal of Neuroscience Methods. 2015; 242:15–40. [PubMed: 25542351]
2. Vazquez AL, et al. Neural and Hemodynamic Responses Elicited by Forelimb- and Photo-stimulation in Channelrhodopsin-2 Mice: Insights into the Hemodynamic Point Spread Function. Cerebral cortex. 2013 Jun 12.
3. Collinger JL, et al. High-performance neuroprosthetic control by an individual with tetraplegia. Lancet. 2012 Dec 13; 381(9866):557–564. [PubMed: 23253623]
4. Hochberg LR, et al. Reach and grasp by people with tetraplegia using a neurally controlled robotic arm. Nature. 2012 May 17.485:372–375. [PubMed: 22596161]
5. Kozai TDY, et al. Brain Tissue Responses to Neural Implants Impact Signal Sensitivity and Intervention Strategies. ACS Chemical Neuroscience. 2015
6. Kozai TDY, et al. In vivo two photon microscopy reveals immediate microglial reaction to implantation of microelectrode through extension of processes. J Neural Eng. 2012; 9:066001. [PubMed: 23075490]
7. Kozai TDY, et al. Reduction of neurovascular damage resulting from microelectrode insertion into the cerebral cortex using in vivo two-photon mapping. J Neural Eng. 2010 Aug.7:046011. [PubMed: 20644246]
8. Seymour JP, Kipke DR. Neural probe design for reduced tissue encapsulation in CNS. Biomaterials. 2007 Sep.28:3594–3607. [PubMed: 17517431]
9. Kozai TDY, et al. Ultrasmall implantable composite microelectrodes with bioactive surfaces for chronic neural interfaces. Nature materials. 2012 Dec.11:1065–1073. [PubMed: 23142839]
10. Kozai TDY, et al. Effects of caspase-1 knockout on chronic neural recording quality and longevity: Insight into cellular and molecular mechanisms of the reactive tissue response. Biomaterials. 2014; 35:9620–9634. [PubMed: 25176060]
11. Kolarcik CL, et al. Elastomeric and soft conducting microwires for implantable neural interfaces. Soft matter. 2015
12. Ludwig KA, et al. Poly(3,4-ethylenedioxythiophene) (PEDOT) polymer coatings facilitate smaller neural recording electrodes. J Neural Eng. 2011 Feb.8:014001. [PubMed: 21245527]
13. Ludwig KA, et al. Chronic neural recordings using silicon microelectrode arrays electrochemically deposited with a poly(3,4-ethylenedioxythiophene) (PEDOT) film. J Neural Eng. 2006 Mar.3:59–70. [PubMed: 16510943]
14. Cui X, Martin DC. Electrochemical deposition and characterization of poly (3, 4-ethylenedioxythiophene) on neural microelectrode arrays. Sensors and Actuators B: Chemical. 2003; 89:92–102. 2003.

15. Cui X, Martin DC. Fuzzy gold electrodes for lowering impedance and improving adhesion with electrodeposited conducting polymer films. Sensors and Actuators A: Physical. 2003; 103:384–394.
16. Cui XY, et al. Electrochemical deposition and characterization of conducting polymer polypyrrole/PSS on multichannel neural probes. Sensors and Actuators a-Physical. 2001 Aug 25.93:8–18.
17. Patel PR, et al. Insertion of linear 8.4 μ m diameter 16 channel carbon fiber electrode arrays for single unit recordings. Journal of Neural Engineering. 2015; 12:046009. [PubMed: 26035638]
18. Kozai, T., et al. Nanostructured coatings for improved charge delivery to neurons. In: Vittorio, MD.; Martiradonna, L.; Assad, J., editors. Nanotechnology and neuroscience: nanoelectronic, photonic and mechanical neuronal interfacing. New York, NY: Springer New York; 2014. p. 71-134.
19. Luo X, et al. Highly stable carbon nanotube doped poly(3,4-ethylenedioxythiophene) for chronic neural stimulation. Biomaterials. 2011 Aug.32:5551–5557. [PubMed: 21601278]
20. Cui XT, Zhou DD. Poly (3,4-ethylenedioxythiophene) for chronic neural stimulation. IEEE Trans Neural Syst Rehabil Eng. 2007 Dec.15:502–508. [PubMed: 18198707]
21. Kolarcik CL, et al. Evaluation of poly(3,4-ethylenedioxythiophene)/carbon nanotube neural electrode coatings for stimulation in the dorsal root ganglion. Journal of Neural Engineering. 2015; 12:016008. [PubMed: 25485675]
22. Mandal HS, et al. Improving the performance of poly(3,4-ethylenedioxythiophene) for brain–machine interface applications. Acta Biomaterialia. 2014; 10:2446–2454. [PubMed: 24576579]
23. Gerwig R, et al. PEDOT–CNT Composite Microelectrodes for Recording and Electrostimulation Applications: Fabrication, Morphology, and Electrical Properties. Frontiers in Neuroengineering. 2012; 5:2012.
24. Hiura H, et al. Opening and purification of carbon nanotubes in high yields. Advanced Materials. 1995; 7:275–276.
25. Qing B, Wise KD. Single-unit neural recording with active microelectrode arrays. Biomedical Engineering, IEEE Transactions on. 2001; 48:911–920.
26. Brainard DH. The Psychophysics Toolbox. Spatial vision. 1997; 10:433–436. [PubMed: 9176952]
27. Pelli DG. The VideoToolbox software for visual psychophysics: transforming numbers into movies. Spatial vision. 1997; 10:437–442. [PubMed: 9176953]
28. Kleiner M, et al. What's new in Psychtoolbox-3? Perception. 2007; 36 p. ECVP Abstract Supplement.
29. Ludwig KA, et al. Using a common average reference to improve cortical neuron recordings from microelectrode arrays. J Neurophysiol. 2009 Mar.101:1679–1689. [PubMed: 19109453]
30. Wagenaar DA, Potter SM. Real-time multi-channel stimulus artifact suppression by local curve fitting. Journal of Neuroscience Methods. 2002 Oct 30.120:113–120. [PubMed: 12385761]
31. Fee MS, et al. Automatic sorting of multiple unit neuronal signals in the presence of anisotropic and non-Gaussian variability. Journal of Neuroscience Methods. 1996 Nov.69:175–188. [PubMed: 8946321]
32. Kozai TDY, et al. Mechanical failure modes of chronically implanted planar silicon-based neural probes for laminar recording. Biomaterials. 2015; 37:25–39. [PubMed: 25453935]
33. Ward MP, et al. Toward a comparison of microelectrodes for acute and chronic recordings. Brain Res. 2009 Jul 28.1282:183–200. [PubMed: 19486899]
34. Prasad A, et al. Abiotic-biotic characterization of Pt/Ir microelectrode arrays in chronic implants. Frontiers in neuroengineering. 2014; 7:2. [PubMed: 24550823]
35. Sankar V, et al. Electrode impedance analysis of chronic tungsten microwire neural implants: understanding abiotic vs. biotic contributions. Frontiers in neuroengineering. 2014; 7:13. [PubMed: 24847248]
36. Karumbaiah L, et al. Relationship between intracortical electrode design and chronic recording function. Biomaterials. 2013 Nov.34:8061–8074. [PubMed: 23891081]

37. Cannizzaro, C., et al. Practical Aspects of Cardiac Tissue Engineering With Electrical Stimulation. In: Hauser, H.; Fussenegger, M., editors. Tissue Engineering. Vol. 140. Humana Press; 2007. p. 291-307.
38. Kozai TDY, Vazquez AL. Photoelectric artefact from optogenetics and imaging on microelectrodes and bioelectronics: New Challenges and Opportunities. Journal of Materials Chemistry B. 2015 vol. *(accepted: in press)*.
39. Luo X, et al. Carbon nanotube nanoreservior for controlled release of anti-inflammatory dexamethasone. Biomaterials. 2011 Sep.32:6316–6323. [PubMed: 21636128]

Biographies

Takashi D.Y. Kozai received a B.A. Magna Cum Laude with Distinction in Molecular, Cellular, and Developmental Biology, and another B.A. with Distinction in Biochemistry from the University of Colorado, Boulder in 2005. He earned his M.S. (2007) and PhD (2011) degree in Biomedical Engineering from the University of Michigan, Ann Arbor. From 2007 to 2009 he also co-founded Fontis Biotechnologies a medical device startup for transdermal macromolecular drug delivery.

From 2011 to 2013, he was a postdoctoral associate in the Department of Bioengineering at University of Pittsburgh. In 2013, he was appointed to Bioengineering to Research Assistant Professor. His primary interests include the areas of elucidating molecular and cellular pathways of brain injuries and diseases, implantable medical devices, biomaterials, and neurotechnology.

Kasey Catt received the B.S.E degree in Bioengineering in 2010 from the Pennsylvania State University, State College. He is currently working toward the Ph.D. degree at the University of Pittsburgh, Pittsburgh.

His current research interests include the use of conductive polymer composites as coatings for improved performance of implantable devices.

Zhanhong Du was born in Xi'an, China, in 1988. He received the B.S. degree in Biological Sciences from the University of Science and Technology of China, Hefei, China, in 2009.

In 2009, he joined the Department of Bioengineering, University of Pittsburgh, as a Ph. D. candidate. His current research interests include conducting polymers, multi-electrode arrays and cortical neural networks.

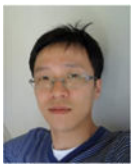

Kyounghwan Na received a B.S. degree in Mechanical Engineering from Seoul National University (Seoul, Korea) in 2005, and a M.S. degree in Electrical Engineering from Seoul National University in 2007. From 2007 to 2011, he had worked for Korea Institute of Science and Technology. Currently, he is pursuing a Ph.D. in Electrical Engineering at the University of Michigan, and his research area is silicon based microfabricated neural probe.

Onnop Srivannavit received the B.S. degree in chemical technology and the M.S. degree in petrochemical technology from Chulalongkorn University, Bangkok, Thailand, and the Ph.D. degree in chemical engineering from the University of Michigan, Ann Arbor, MI in 2002. He was a research engineer at the University of Michigan from 2002 to 2012. He is currently a lead engineer at ePack, Ann Arbor MI. His research interests include the development of microelectromechanical systems and microfluidic devices for biomedical and environmental applications.

Razi-ul Haque received BSE degrees in both Electrical Engineering and Computer Engineering from the University of Michigan, Ann Arbor in 2004. He received the MSE degree in Electrical Engineering in 2005 and a PhD in Electrical Engineering: Circuits & Microsystems in 2011, all from the University of Michigan, Ann Arbor. Since 2001, he has worked on a variety of microelectromechanical systems, from microfluidic devices for DNA analysis to a highly-integrated and compact microsystem for in-vivo continuous monitoring. During his postdoctoral work at the University of Michigan, he explored neural probe designs that reduced neural tissue damage by minimizing silicon area. Dr. Haque is currently the President & CEO of Structured Microsystems LLC, a spinoff from the University of

Michigan that is specializing in microsystem design and especially on products based on the proprietary glass-in-silicon reflow process that he developed during his graduate work. His main area of interest is in implantable BioMEMS and novel microfabrication techniques that enable new microsystems for interdisciplinary solutions.

John Seymour earned his B.S. with Honors in Engineering Physics from Ohio State University, M.S. (2004) and Ph.D (2009) in Biomedical Engineering at the University of Michigan. He is currently a Senior Research Fellow in the Department of Electrical Engineering at the University of Michigan. He worked at NeuroNexus, a neurotechnology firm, from 2009 to 2013. His research interests are in MEMS, electrophysiological sensors, implantable medical devices, optical stimulation tools, and advanced packaging.

Kensall D. Wise received the BSEE degree with highest distinction from Purdue University in 1963 and the MS and Ph.D. degrees in electrical engineering from Stanford University in 1964 and 1969, respectively. From 1963 to 1965 and from 1972 to 1974, he was a Member of Technical Staff at Bell Telephone Laboratories, where his work focused on the exploratory development of integrated electronics for use in telephone communications. From 1965 to 1972 he was a Research Assistant and then a Research Associate and Lecturer at Stanford, working on the development of micromachined silicon sensors. In 1974 he joined the University of Michigan, Ann Arbor, where he is now the William Gould Dow Distinguished University Professor Emeritus of Electrical Engineering and Computer Science and Professor Emeritus of Biomedical Engineering. Dr. Wise was General Chairman of the 1984 IEEE Solid-State Sensor Conference (Hilton Head) and was Technical Program Chairman (1985) and General Chairman (1997) of the IEEE International Conference on Solid-State Sensors, Actuators, and Microsystems. He received the 1990 Paul Rappaport Award from the IEEE Electron Devices Society, the 1995 Distinguished Faculty Achievement Award from the University of Michigan, the 1996 Columbus Prize from the Christopher Columbus Fellowship Foundation, the 1997 SRC Aristotle Award, and the 1999 IEEE Solid-State Circuits Technical Field Award. He held the 2007 Henry Russel Lectureship at the University of Michigan and is a Life Fellow of the IEEE, a Fellow of the AIMBE, and a member of the United States National Academy of Engineering.

Euisik Yoon received the B.S. and M.S. degrees in electronics engineering from Seoul National University, Seoul, Korea, in 1982 and 1984, respectively, and the Ph.D. degree in electrical engineering from the University of Michigan, Ann Arbor, in 1990. From 1990 to 1994, he worked for the Fairchild Research Center of the National Semiconductor Corporation, Santa Clara, CA, where he engaged in researching deep submicron CMOS integration and advanced gate dielectrics. From 1994 to 1996, he was a Member of the Technical Staff at Silicon Graphics Inc., Mountain View, CA, where he worked on the design of the MIPS microprocessor R4300i and the RCP 3-D graphic coprocessor. He took faculty positions in the Department of Electrical Engineering, Korea Advanced Institute of Science and Technology (KAIST), Daejeon, Korea, from 1996 to 2005, and in the Department of Electrical and Computer Engineering, University of Minnesota, Minneapolis, from 2005 to 2008, respectively. During the academic year of 2000 to 2001, he was a Visiting Faculty at Agilent Laboratory, Palo Alto, CA. In 2008, he joined the Department of Electrical Engineering and Computer Science, University of Michigan, Ann Arbor, where he is a Professor and is currently serving as the Director of the Lurie Nanofabrication Facility. His research interests are in MEMS, integrated microsystems, and VLSI circuit design.

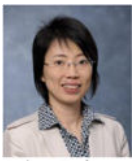

Xinyan Tracy Cui was born in Beijing, China in 1971. She received the B.E. degree in Polymer Materials and Chemical Engineering and M.S. degree in Biophysics from Tsinghua University, Beijing, China in 1994 and 1997 respectively. She then obtained her Ph.D. in Macromolecular science and engineering from University of Michigan, Ann Arber, in 2002. In 2003, she joined the Department of Bioengineering, University of Pittsburgh, as an Assistant Professor, and became full Professor in 2015. Her research interests lie in neural engineering with special focuses on neural electrode-tissue interface, neural tissue engineering, CNS drug delivery and biosensor. Specific projects include: 1) Biomimetic surface coatings for neural microelectrode arrays to improve chronic neural recording and stimulation stability, reliability and longevity; 2) Micro-patterning of biochemical, surface chemical and electrical cues on electrode arrays for neural network study; 3) Controlled drug delivery and biochemical sensing in nervous system; 4) Control of neural stem cell growth and differentiation via surface and electrical cues. She is the associate editor of Journal of Materials Chemistry B and recipients of Wallace Coulter Foundation Early Career Award (2005), National Science Foundation Career Award (2008) and Carnegie Science Award Emerging Female Scientist (2013).

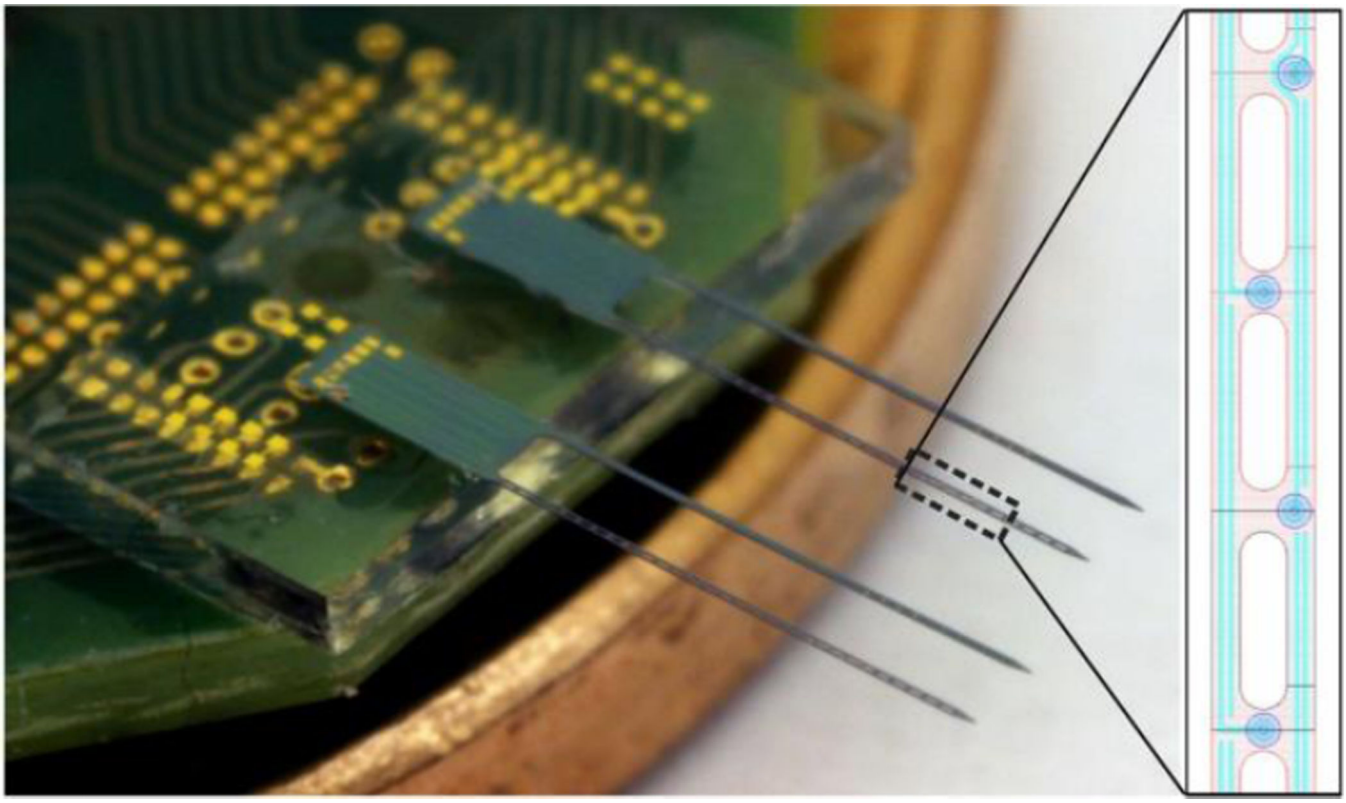

Figure 1.
Dual shank silicon neural probe was fabricated using deep boron doping, polysilicon interconnects, and evaporated Au microelectrodes. In each dual shank probe, one shank had an open lattice design and the other was solid, both having identical electrode layouts (inset).

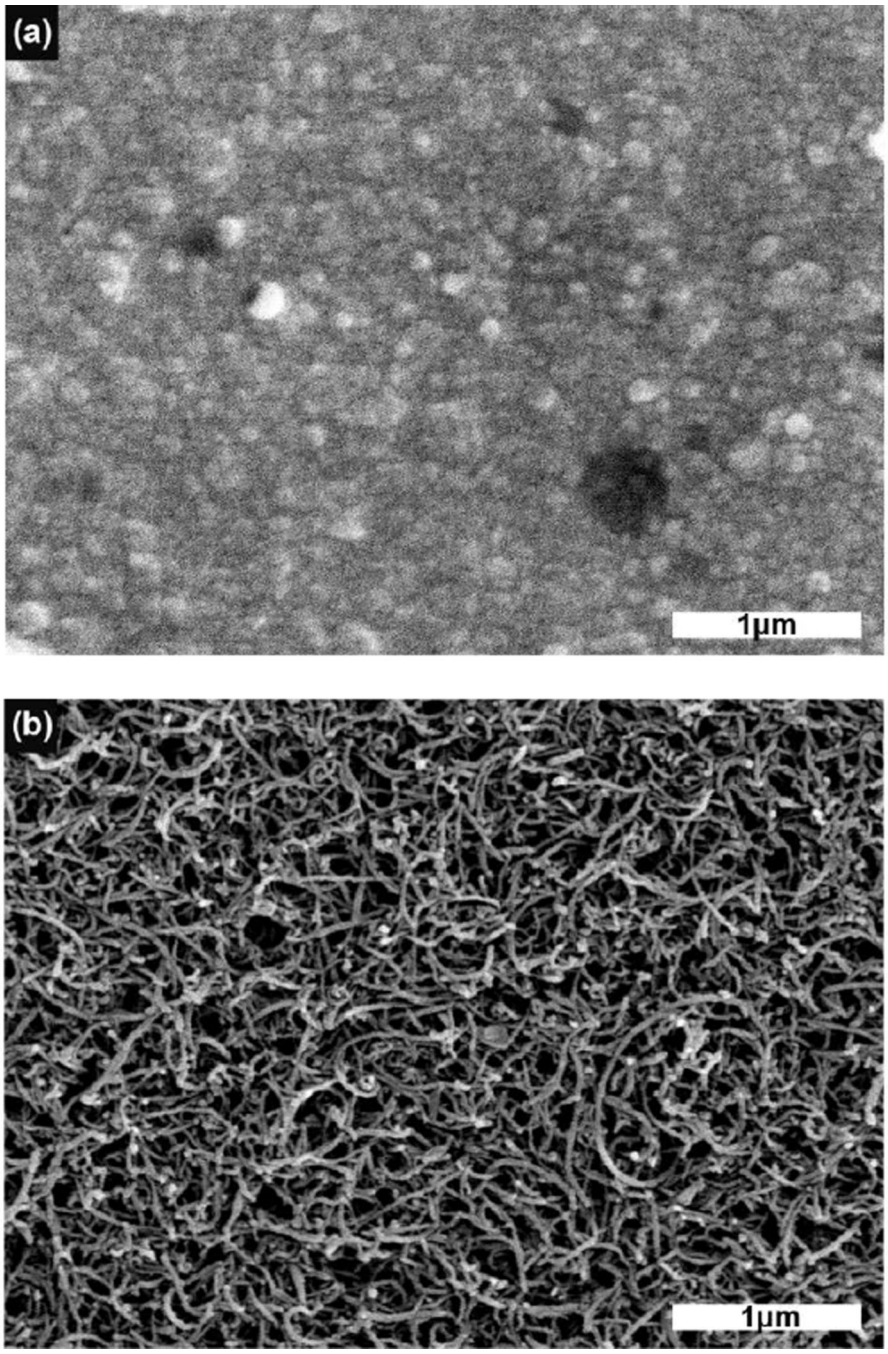

Figure 2.
Scanning electron microscopy images of (a) PEDOT/PSS coated recording sites, and (b) PEDOT/CNT-$(COOH)_x$ coated recording sites.

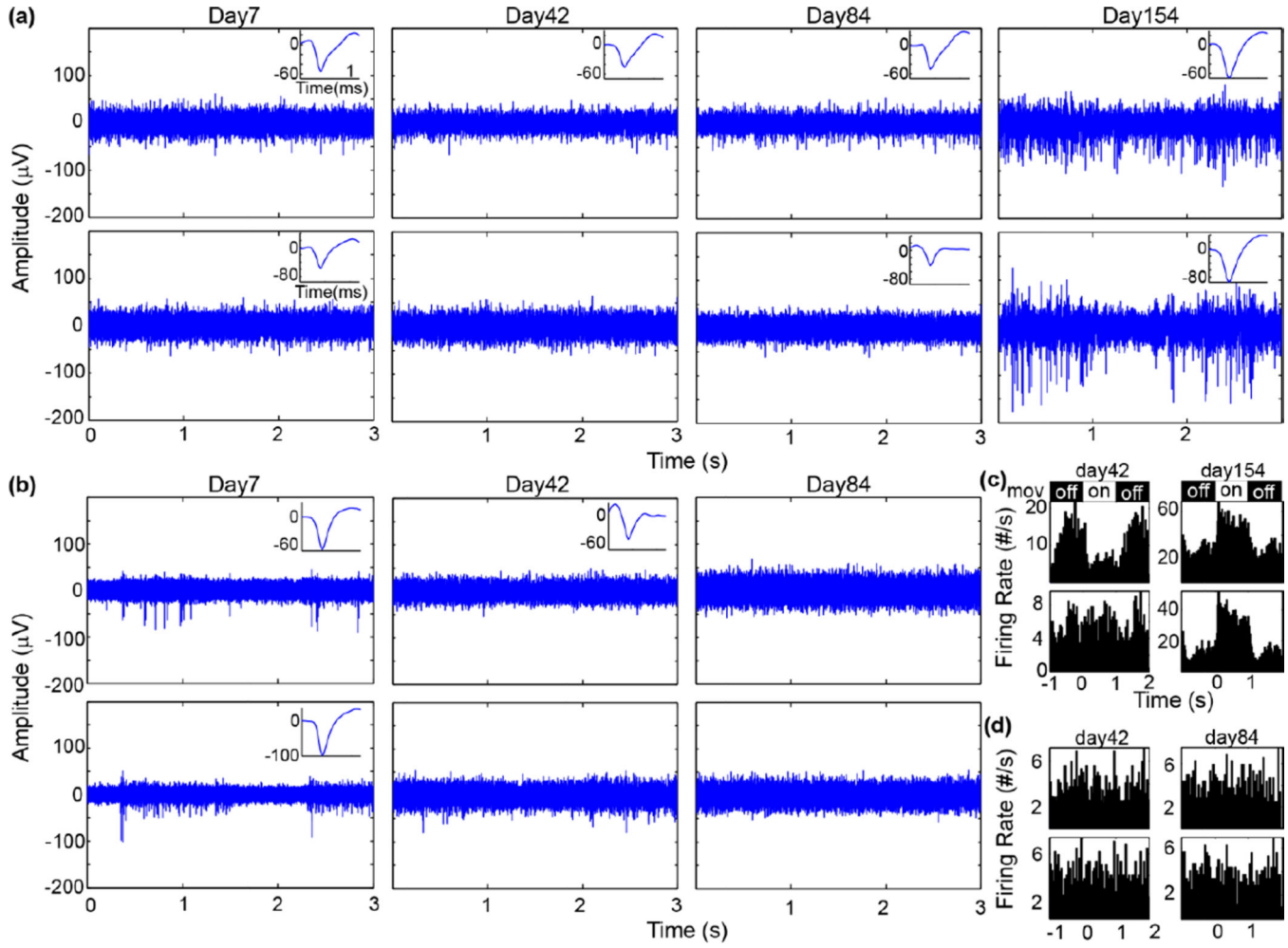

Figure 3.

Example chronic spike recordings. (a–b) Raw spike stream (300–5,000Hz) from PEDOT/CNT-$(COOH)_x$ sites (a) and PEDOT/PSS sites (b) over time. Insets show isolated single-unit waveform in a 1.2 ms window. (c–d) Peristimulus time histogram (50 ms bins) of visually evoked threshold crossings from PEDOT/CNT-$(COOH)_x$ sites (a) and PEDOT/PSS sites (b) over time. Drifting gratings (mov) were displayed (on) from 0 for 1s followed by 1 s of black screen (off).

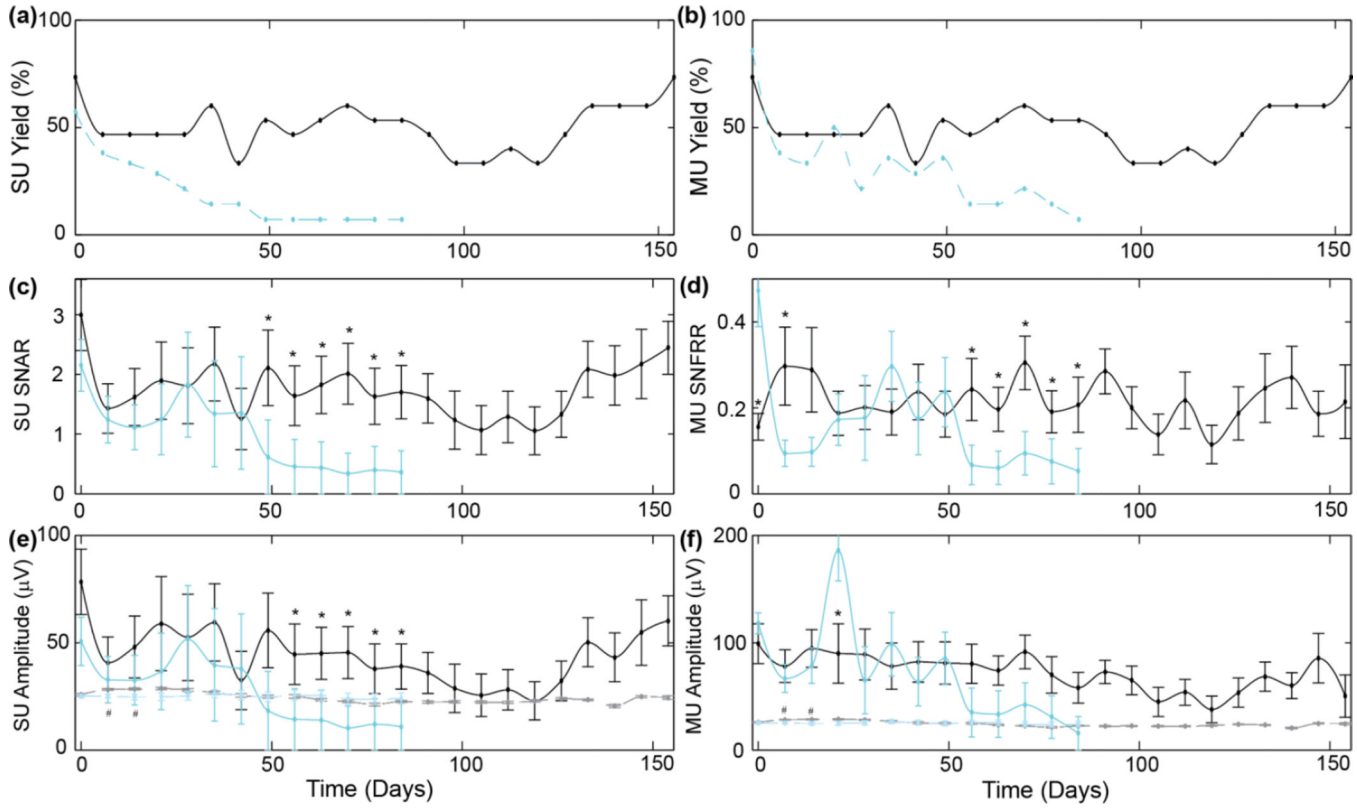

Figure 4.

Chronic spike recording performance of PEDOT/CNT-$(COOH)_x$ (black) and PEDOT/PSS (blue) electrode sites. (a) SU yield, (b) MU yield. (c) SU signal-to-noise amplitude ratio for the largest isolated SU waveform. (d) Visually evoked MU signal-to-noise firing rate ratio. (e) Average amplitude of the largest SU waveform on each channel (solid line). (f) Average MU amplitude (solid line). (e–f) dashed line indicates noise floor. * indicates significant difference of SNR or Amplitude ($p<0.05$). # indicates significant difference in noise floor ($p<0.05$). Note: If no SU or MU were detected, SNR=0 and amplitude=0 μV. Average SU SNAR and SU amplitude may be lower than the noise floor if large number of recording sites had SNR=0 and amplitude=0 μV. As previously published, this was done to prevent misleading over characterization of 'AVERAGE SNR' by ignoring or removing 'failed' recording sites during averaging.

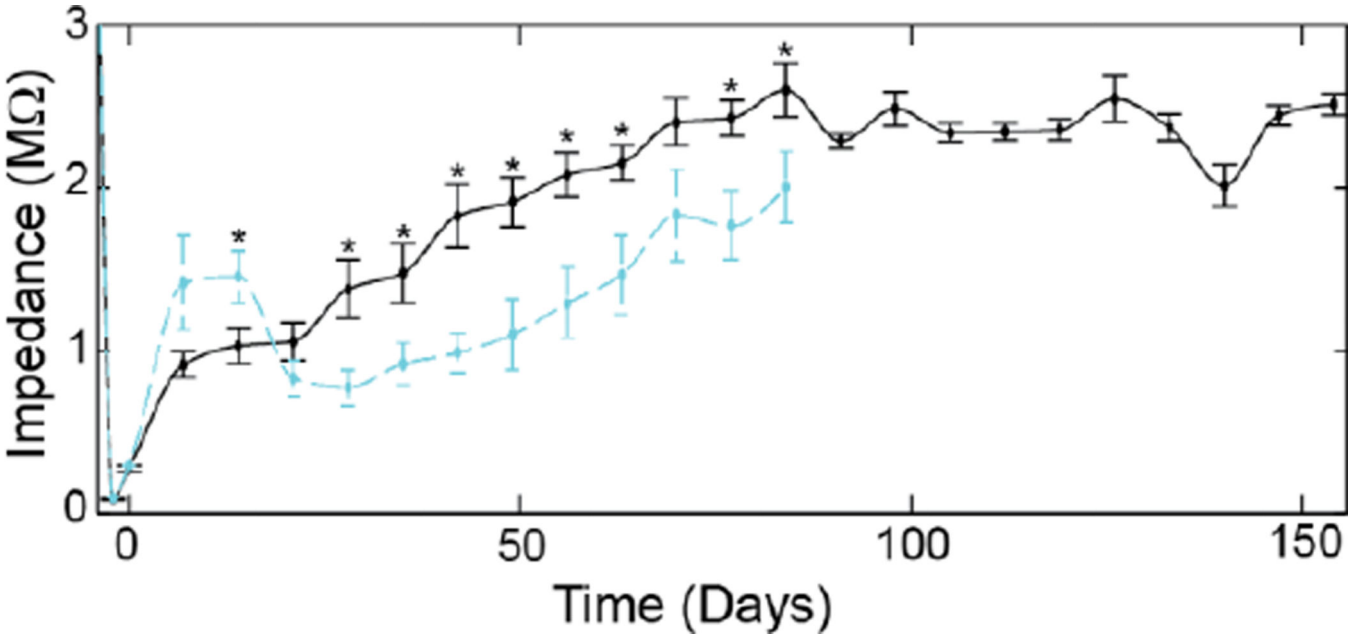

Figure 5.

1kHz impedance of PEDOT/PSS (cyan) and PEDOT/CNT (black). * indicates significant difference (p<0.05). Note: −4 day time point indicates uncoated Au electrode and −2 day time point indicates coated electrodes prior to surgery.